The Drosophila Baramicin polypeptide gene protects against fungal infection

M.A. Hanson[1*], L.B. Cohen[2], A. Marra[1], I. Iatsenko[1,3], S.A. Wasserman[2], and B. Lemaitre[1]

1 Global Health Institute, School of Life Science, École Polytechnique Fédérale de Lausanne (EPFL), Lausanne, Switzerland.
2 Division of Biological Sciences, University of California San Diego (UCSD), La Jolla, California, United States of America.
3 Max Planck Institute for Infection Biology, 10117, Berlin, Germany.
* Corresponding author: M.A. Hanson (mark.hanson@epfl.ch), B. Lemaitre (bruno.lemaitre@epfl.ch)

ORCID IDs:
Hanson: https://orcid.org/0000-0002-6125-3672
Cohen: https://orcid.org/0000-0002-6366-570X
Iatsenko: https://orcid.org/0000-0002-9249-8998
Wasserman: https://orcid.org/0000-0003-1680-3011
Lemaitre: https://orcid.org/0000-0001-7970-1667

Abstract

The fruit fly *Drososphila melanogaster* combats microbial infection by producing a battery of effector peptides that are secreted into the haemolymph. Technical difficulties prevented the investigation of these short effector genes until the recent advent of the CRISPR/CAS era. As a consequence, many putative immune effectors remain to be characterized and exactly how each of these effectors contributes to survival is not well characterized. Here we describe a novel *Drosophila* antifungal peptide gene that we name *Baramicin A*. We show that *BaraA* encodes a precursor protein cleaved into multiple peptides via furin cleavage sites. *BaraA* is strongly immune-induced in the fat body downstream of the Toll pathway, but also exhibits expression in the nervous system. Importantly, we show that flies lacking *BaraA* are viable but susceptible to the enomopathogenic fungus *Beauveria bassiana*. Consistent with *BaraA* being directly antimicrobial, overexpression of *BaraA* promotes resistance to fungi and the IM10-like peptides produced by *BaraA*

synergistically inhibit growth of fungi in vitro when combined with a membrane-disrupting antifungal. Surprisingly, *BaraA* males but not females display an erect wing phenotype upon infection. Collectively, we identify a new antifungal immune effector downstream of Toll signalling, improving our knowledge of the *Drosophila* antimicrobial response.

Introduction

The innate immune response provides the first line of defence against pathogenic infection. This reaction is usually divided into three stages: i) the recognition of pathogens through dedicated pattern recognition receptors, ii) the activation of conserved immune signalling pathways and iii) the production of immune effectors that target invading pathogens [1,2]. The study of invertebrate immune systems has led to key observations of broad relevance, such as the discovery of phagocytosis [3], antimicrobial peptides (AMPs) [4], and the implication of Toll receptors in metazoan immunity [5]. Elucidating immune mechanisms, genes, and signalling pathways has greatly benefited from investigations in the fruit fly *Drosophila melanogaster*, which boasts a large suite of molecular and genetic tools for manipulating the system. One of the best-characterized immune reactions of *Drosophila* is the systemic immune response. This reaction involves the fat body (an analog of the mammalian liver) producing immune effectors that are secreted into the haemolymph. In *Drosophila*, two NF-κB signalling pathways, the Toll and Imd pathways, regulate most inducible immune effectors: the Toll pathway is predominantly activated in response to infection by Gram-positive bacteria and fungi [5,6], while the immune-deficiency pathway (Imd) responds to the DAP-type peptidoglycan most commonly found in Gram-negative bacteria and a subset of Gram-positive bacteria [7]. These two signalling pathways regulate a transcriptional program that results in the massive synthesis and secretion of humoral effector peptides [6,8]. Accordingly, mutations affecting the Toll and Imd pathways cause extreme susceptibilities to systemic infection that reflect the important contribution of these pathways to host defence. The best-

67 characterized immune effectors downstream of these pathways are antimicrobial
68 peptides (AMPs). AMPS are small and often cationic peptides that disrupt the
69 membranes of microbes, although some have more specific mechanisms [9].
70 Multiple AMP genes belonging to seven well-characterized families are induced
71 upon systemic infection [10]. However transcriptomic analyses have revealed that
72 the systemic immune response encompasses far more than just the canonical AMPs.
73 Many uncharacterized genes encoding small secreted peptides are induced to high
74 levels downstream of the Toll and Imd pathways, pointing to the role for these
75 peptides as immune effectors [11]. In parallel, MALDI-TOF analyses of the
76 haemolymph of infected flies revealed the induction of 24 peaks - mostly
77 corresponding to uncharacterized peptides - that were named "IMs" for Immune-
78 induced Molecules (IM1-IM24) [8]. Many of the genes that encode these components
79 of the immune peptidic secretome have remained largely unexplored. This is mainly
80 due to the fact that these IMs belong to large gene families of small genes that were
81 until recently difficult to disrupt by mutagenesis.
82
83 The CRISPR/Cas9 gene editing approach now allows the necessary precision
84 to delete small genes, singly or in groups, providing the opportunity to dissect
85 effector peptide functions. In 2015 a family of 12 related IM-encoding genes, unified
86 under the name *Bomanins*, were shown to function downstream of Toll. Importantly,
87 a deletion removing 10 out of the 12 Bomanins revealed their potent contribution to
88 defence against both Gram-positive bacteria and fungi [12]. While Bomanins
89 contribute significantly to Toll-mediated defence, their molecular functions are still
90 unknown and it is unclear if they are directly antimicrobial [13]. Two other IMs
91 encoding IM4 and IM14 (renamed *Daisho1* and *Daisho2*, respectively) were shown
92 to contribute downstream of Toll to resistance against specific fungi. Interestingly,
93 Daisho peptides bind to fungal hyphae, suggesting direct antifungal activity [14].
94 Finally a systematic knock-out analysis of *Drosophila* AMPs revealed that they play
95 an important role in defence against Gram-negative bacteria and some fungi, but
96 surprisingly little against Gram-positive bacteria [15]. An unforeseen finding from
97 these recent studies is the high degree of AMP-pathogen specificity: this is perhaps

98 best illustrated by the specific requirement for *Diptericin*, but not other AMPs, in
99 defence against *Providencia rettgeri* [15,16]. Collectively, these studies in *Drosophila*
100 reveal that immune effectors can be broad or specific in mediating host-pathogen
101 interactions. Understanding the logic of the *Drosophila* effector response will thus
102 require a careful dissection of the remaining uncharacterized immune induced
103 peptides.
104
105 Previous studies identified an uncharacterized Toll-regulated gene called
106 *IMPPP/CG33470*, which we rename "*BaraA*" (see below), that encodes several IMs,
107 indicating a role in the humoral response. Here, we have improved the annotation of
108 IMs produced by *BaraA* to include: IM10, IM12 (and its sub-peptide IM6), IM13 (and
109 its sub-peptides IM5 and IM8), IM22, and IM24. Using a *BaraA* reporter, we show
110 that *BaraA* is not only immune-induced in the fat body, but also expressed in the
111 head, and nervous system tissue including the eyes, and ocelli. Importantly, we show
112 that flies lacking *BaraA* are viable but susceptible to specific infections, notably by
113 the entomopathogenic fungus *Beauveria bassiana*. Consistent with this, the IM10-
114 like peptides produced by *BaraA* inhibit fungal growth in vitro when combined with
115 the antifungal Pimaricin. Surprisingly, *BaraA* deficient males also display a striking
116 erect wing behaviour upon infection. Collectively, we identify a new antifungal
117 immune effector downstream of Toll signalling, improving our knowledge of the
118 *Drosophila* antimicrobial response.
119

120 Results:

121

122 *BaraA is regulated by the Toll pathway*

123

124 Previous microarray studies from De Gregorio et al. [11] suggest that *BaraA* is
125 primarily regulated by the Toll pathway, with a minor input from the Imd pathway
126 (**Fig.** 1A). Consistent with this, we found several putative NF-κB binding sites
127 upstream of the *BaraA* gene (guided by previous reports [17–19]). Notably there are

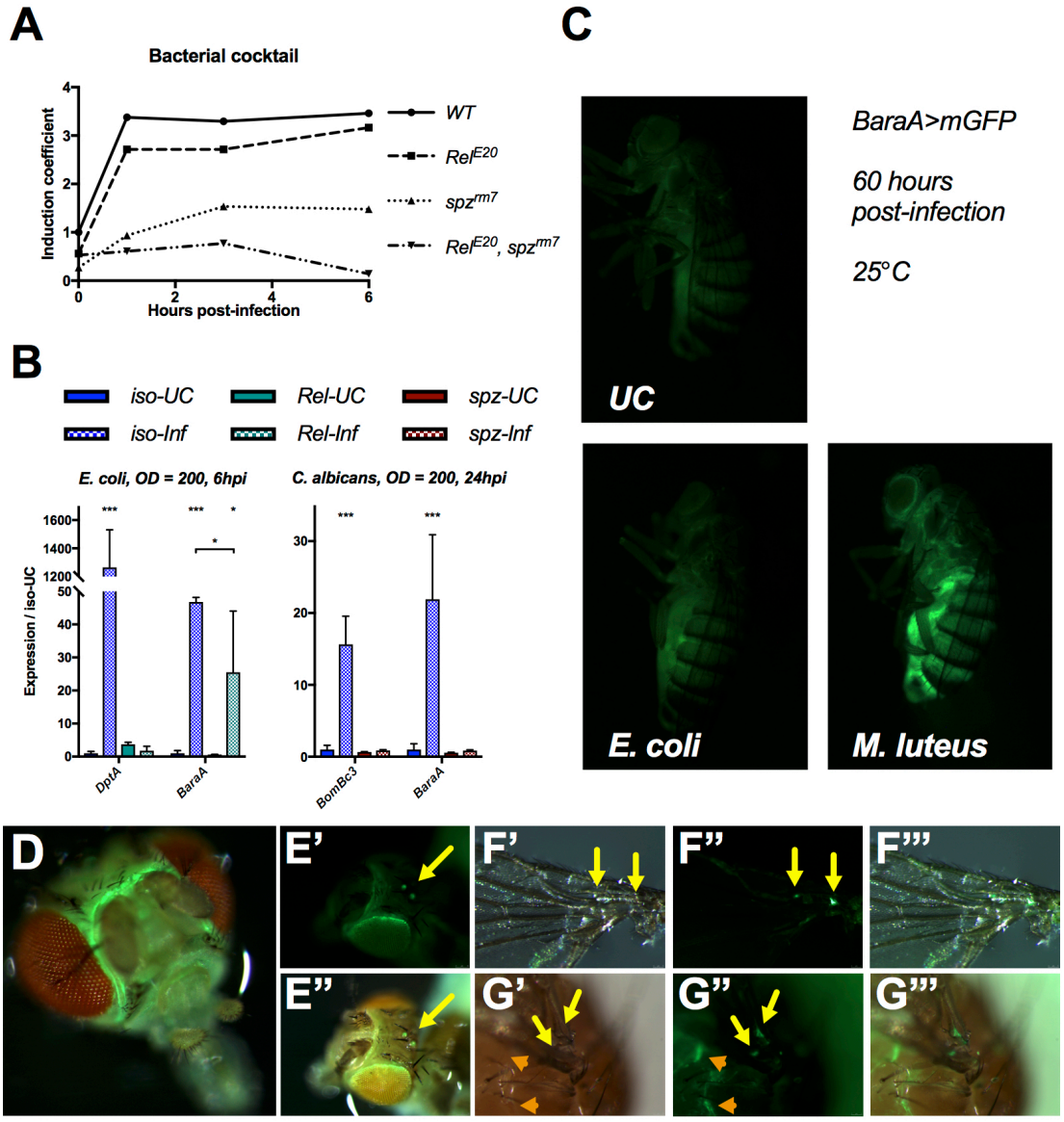

Figure 1: *BaraA* is an immune-induced gene regulated by the Toll pathway. A) Expression profile of *BaraA* upon bacterial challenge by a mixture of *E. coli* and *M. luteus* (from De Gregorio et al. [11]). Induction coefficient is a complex calculation of log-fold change reported in De Gregorio et al. [11], and values are given relative to wild type unchallenged expression levels. B) *BaraA* expression profiles in wild-type, spz^{rm7} and Rel^{E20} flies upon septic injury with the Gram-negative bacterium *E. coli* and the yeast *C. albicans*. *DptA* and *BomBc3* were used as inducible control genes for the Imd and Toll pathways respectively. Floating asterisks indicate significance relative to *iso-UC* where: * = $p < .05$ and, *** = $p < .001$. C) Use of a *BaraA* reporter reveals that *BaraA* induction upon infection is primarily driven by the fat body in adults, and results in a much stronger GFP signal upon pricking with *M. luteus* (which stimulates the Toll pathway) compared to *E. coli* (which stimulates the Imd pathway). Representative images taken 60h (adults) after handling alone (UC) or infection with *E. coli* or *M. luteus* (OD=200). D-G) *BaraA>mGFP* is highly expressed in the head (D), at the border of the eyes and in the ocelli (E), in the wing veins (F-G yellow arrows), and beneath the cuticle in the thorax (H, orange arrows).

144 two putative binding sites for Relish, the transcription factor of the Imd pathway
145 and three putative binding sites for the Dif/Dorsal transcription factors acting
146 downstream of Toll (**Fig.** S1A). We challenged wild type flies and Imd or Toll
147 pathway mutants (*Rel*^{E20} and *spz*^{rm7} respectively) with the Gram-negative bacterium
148 *Escherichia coli*, the yeast *Candida albicans*, or the Gram-positive bacterium
149 *Micrococcus luteus*. RT-qPCR analysis confirms that *BaraA* is induced by infection
150 with *E. coli*, *C. albicans*, or *M. luteus (***Fig.** 1B and **Fig.** S1B). *BaraA* remains highly
151 inducible in a *Relish* mutant background, albeit at slightly reduced level compared to
152 the wild type. However *BaraA* expression is abolished in *spz*^{rm7} flies. Collectively, the
153 expression pattern of *BaraA* is reminiscent of the antifungal peptide gene
154 *Drosomycin* with a primary input by the Toll pathway and a minor input from the
155 Imd pathway [10,20].
156
157 To further characterize the expression of *BaraA*, we generated a *BaraA-Gal4*
158 transgene in which 1675bp of the *BaraA* promoter sequence is fused to the yeast
159 transcription factor Gal4. Use of *BaraA-Gal4>UAS-mCD8-GFP* (referred to as
160 *BaraA>mGFP*) reveals that *BaraA* is strongly induced in the fat body 60h post
161 infection by *M. luteus*, but less so by *E. coli* pricking (**Fig.** 1C); dissections confirmed
162 this GFP signal is produced by the fat body. Larvae pricked with *M. luteus* also show
163 a robust GFP signal primarily stemming from the fat body when examined 2hpi (**Fig.**
164 S1C). We also observed a strong constitutive GFP signal in the headcase of adults
165 (**Fig.** 1D), including the border of the eyes and the ocelli (**Fig.** 1E). Dissection
166 confirmed that the *BaraA* reporter is expressed in brain tissue, notably in the central
167 ventral brain furrow. Other consistent signals include GFP in the wing veins and
168 subcutaneously along borders of thoracic pleura in adults (**Fig.** 1F-G), and in
169 spermatheca of females (**Fig.** S1D). There was also sporadic GFP signal in other
170 tissues that included the larval hindgut, the dorsal abdomen of developing pupae,
171 and the seminal vesicle of males. These expression patterns largely agree with data
172 reported in FlyAtlas1 [21].
173
174

175 ***Baramicin A encodes a precursor protein cleaved into multiple peptides***

176

177 Previous studies using bioinformatics and proteomics have suggested that
178 four highly immune-induced peptides (IM10, IM12, IM13, and IM24) are encoded in
179 tandem as a single polypeptide precursor by *IMPPP/BaraA* [8,22]. Some less-
180 abundant sub-peptides (IM5, IM6, and IM8) are also produced by additional
181 cleavage of IM12 and IM13 [22]. Using a newly generated null mutant ("*ΔBaraA,*"
182 described below), we analyzed haemolymph samples of wild type and *ΔBara* flies
183 infected with a bacterial mixture of *E. coli* and *M. luteus* by MALDI-TOF analysis. We
184 confirmed the loss of the seven immune-induced peaks corresponding to IMs 5, 6, 8,
185 10, 12, 13, and 24 in *ΔBaraA* flies (**Fig.** 2A). We also noticed that an additional
186 immune-induced peak at ~5975 Da was absent in our *BaraA* mutants. Upon re-
187 visiting the original studies that annotated the *Drosophila* IMs, we realized this peak
188 corresponded to IM22, whose sequence was never determined [8,22] (see
189 supplementary information for details). We subjected haemolymph from infected
190 flies to LC-MS proteomic analysis following trypsin digestion and found that in
191 addition to the known IMs of *BaraA* (IMs 5, 6, 8, 10, 12, 13, and 24), trypsin-digested
192 fragments of the *BaraA* C-terminus peptide were also detectable in the haemolymph
193 (**Fig.** S2). The range of detected fragments did not match the full length of the C-
194 terminus exactly, as the first four residues were absent in our LC-MS data (a
195 truncation not predicted to arise via trypsin cleavage). The *BaraA* C-terminus
196 lacking these four residues has a calculated mass of 5974.5 Da, exactly matching the
197 observed mass of the IM22 peak absent in *BaraA* mutant flies. Furthermore in other
198 *Drosophila* species these four residues of the *BaraA* C-terminus are instead an RXRR
199 furin cleavage motif (**Fig.** S3A). Therefore IM22 cleavage in other species, even by an
200 alternate cleavage process, should result in the same maturated IM22 domain as
201 found in *D. melanogaster*. Taken together, we conclude that IM22 is the mature form
202 of the BaraA protein C-terminus.

203

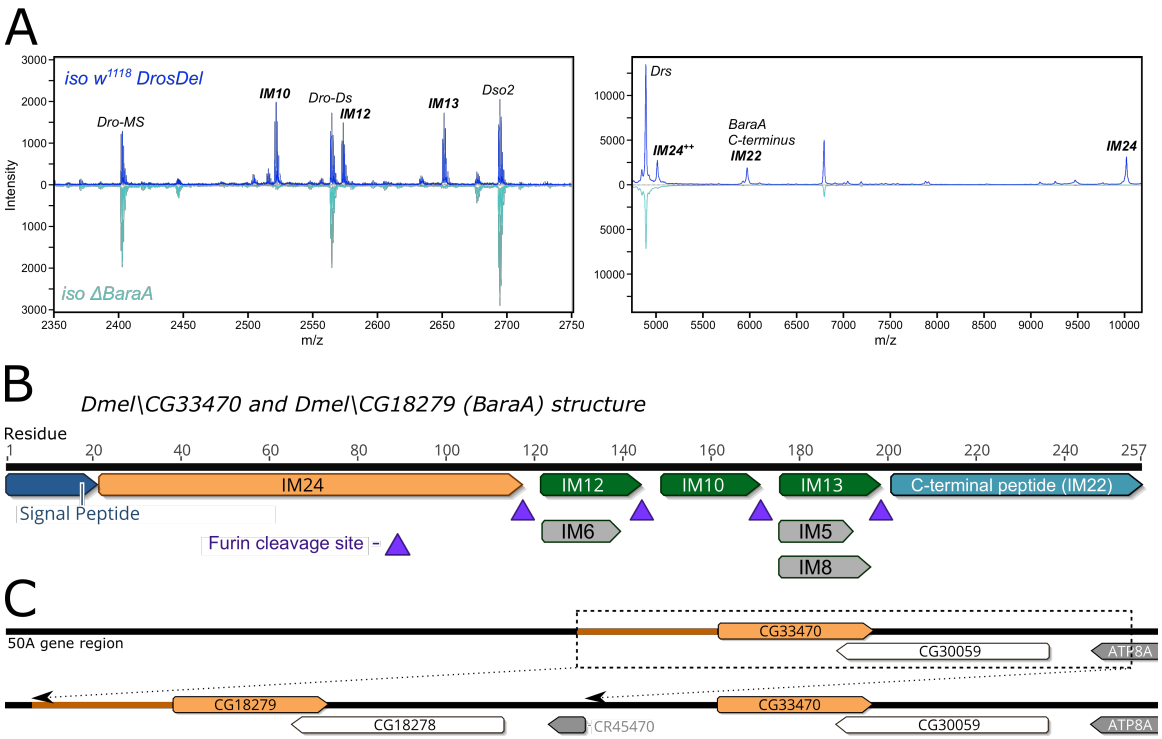

Figure 2: The *BaraA* gene structure. A) MALDI-TOF analysis of haemolymph from *iso w*^{1118} wild-type and *iso ΔBaraA* flies 24 hours post-infection (hpi) confirms that *BaraA* mutants fail to produce the IM10-like and IM24 peptides. *iso ΔBaraA* flies also fail to produce an immune-induced peak at ~5794 Da corresponding to IM22 (the C-terminal peptide of BaraA, see supplementary information). B) The *BaraA* gene encodes a precursor protein that is cleaved into multiple mature peptides at RXRR furin cleavage sites. The sub-peptides IMs 5, 6, and 8 are additional minor cleavage products of IM12 and IM13. IM22 is additionally cleaved following its GIND motif (Fig. S2 and S3A). C) There is a *BaraA* locus duplication event present in the Dmel_R6 reference genome. This duplication is not fixed in laboratory stocks and wild-type flies (Hanson and Lemaitre, 2020; in prep.).

Thus, a single gene, *BaraA*, contributes to one third of the originally described *Drosophila* IMs. These peptides are encoded as a polypeptide precursor interspersed by furin cleavage sites (e.g. RXRR) (**Fig.** 2B). We note that the IM10, IM12 and IM13 peptides are tandem repeats of related peptides, which we collectively refer to as "IM10-like" peptides (**Fig.** S3B). The IM22 peptide also contains a similar motif as the IM10-like peptides (**Fig.** S3A-B), suggesting a related biological activity. We name this gene "*Baramicin A*" (symbol: *BaraA*) for the Japanese idiom Bara Bara (バラバラ), meaning "to break apart;" a reference to the fragmenting structure of the *Baramicin* precursor protein and its many peptidic products.

226 ***A BaraA duplication is present in some laboratory stocks***

227

228 Over the course of our investigation, we realized that *IMPPP (CG18279)* was
229 identical to its neighbour gene *CG33470* owing to a duplication event of the *BaraA*
230 locus present in the *D. melanogaster* reference genome. The exact nature of this
231 duplication is discussed in a separate article (Hanson and Lemaitre; in prep). In
232 brief, the duplication involves the entire *BaraA* gene including over 1kbp of 100%
233 identical promoter sequence, and also the neighbouring sulfatase gene CG30059 and
234 the 3' terminus of the *ATP8A* gene region (**Fig.** 2C). We distinguish the two daughter
235 genes as *BaraA1 (CG33470)* and *BaraA2 (CG18279).* Available sequence data
236 suggests the *BaraA1* and *BaraA2* transcripts are 100% identical. We analyzed the
237 presence of the *BaraA* duplication using a PCR assay spanning the junction of the
238 duplicated region (supplementary data file 1). Interestingly, *BaraA* copy number is
239 variable in common lab strains and wild flies, indicating this duplication event is not
240 fixed in *D. melanogaster* (Hanson and Lemaitre; in prep).

241

242 ***Over-expression of BaraA improves the resistance of immune deficient flies***

243

244 *Imd, Toll* deficient flies are extremely susceptible to microbial infection as
245 they fail to induce hundreds of immune genes, including antimicrobial peptides [11].
246 It has been shown that over-expression of even a single AMP can improve the
247 resistance of *Imd, Toll* deficient flies [23]. As such, immune gene over-expression in
248 *Imd, Toll* immune-compromised flies provides a direct assay to test the ability of a
249 gene to contribute to defence independent of other immune effectors. We applied
250 this strategy to *Baramicin A* by generating flies that constitutively express *BaraA*
251 using the ubiquitous *Actin5C-Gal4* driver *(Act-Gal4)* in an immune-deficient Rel^{E20},
252 spz^{rm7} double mutant background (**Fig.** S4A). In these experiments, we pooled
253 results from both males and females due to the very low availability of homozygous
254 *Rel, spz* adults, particularly when combined with *Act-Gal4*. Overall, similar trends
255 were seen in both sexes, and separate male and female survival curves are shown in
256 **Fig.** S4.

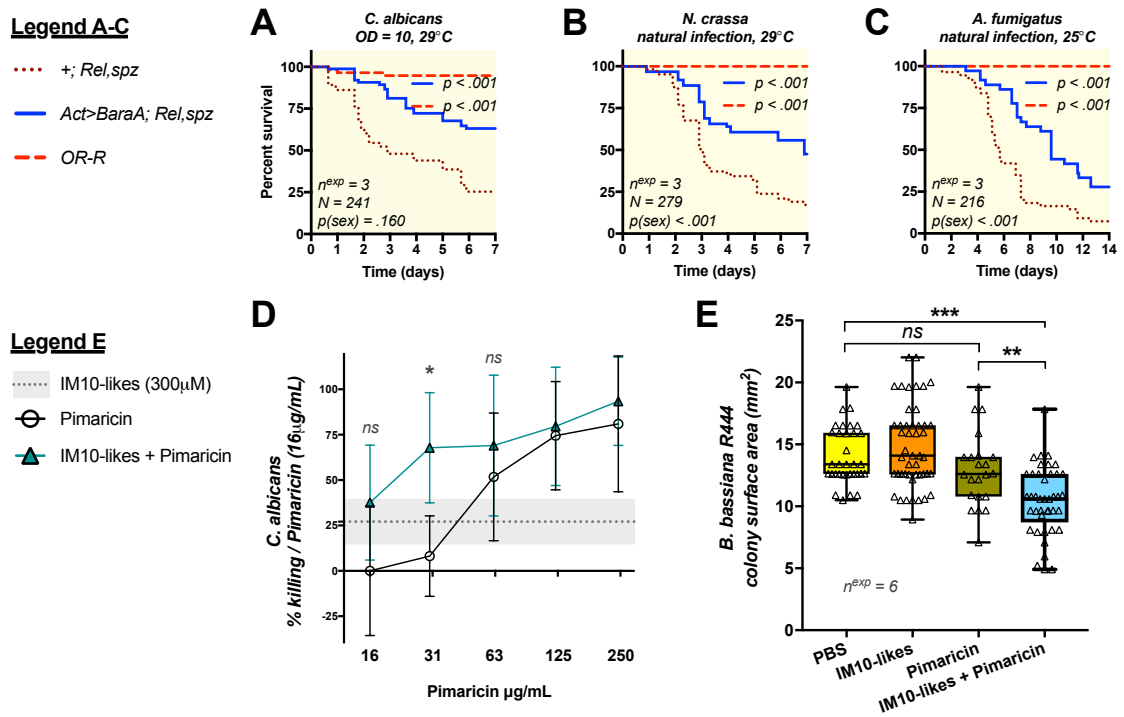

Figure 3: Overexpression of *BaraA* partially rescues the susceptibility of *Rel, spz* flies against fungi and BaraA IM10-like peptides inhibit fungal growth in vitro. A-C) Overexpression of *BaraA* (*Act>BaraA)* rescues the susceptibility of *Rel, spz* flies upon systemic infection with *C. albicans* (A), or natural infection with either *N. crassa* or *A. fumigatus* (B-C). Survivals represent pooled results from males and females (see Fig. S4 for sex-specific survival curves). D) A 300µM cocktail of the three IM10-like peptides improves the killing activity of the antifungal Pimaricin against *C. albicans* yeast. Error bars and the shaded area (IM10-likes alone) represent ±1 standard deviation from the mean. Killing activity (%) was compared against no-peptide controls, then normalized to the activity of Pimaricin alone. E) The IM10-like peptide cocktail also synergizes with Pimaricin to inhibit mycelial growth of *B. bassiana strain R444*. The diameters of individual colonies of *B. bassiana* were assessed after four days of growth at 25°C after peptide treatment, and surface area calculated as πr^2.

Ubiquitous *BaraA* expression marginally improved the survival of *Rel, spz* flies upon infection with *M luteus* bacteria, however there was no effect upon infection with *E. coli* (**Fig. S4B-C**). On the other hand, ubiquitous expression of *BaraA* provided a more pronounced protective effect against infection by a variety of fungal pathogens. This was true upon pricking with *C. albicans* (**Fig.** 3A), or upon natural infections using *Aspergillus fumigatus* or *Neurospora crassa* filamentous fungi (**Fig.** 3B-C). This over-expression study reveals that *BaraA* alone can partially rescue the susceptibility of *Imd, Toll* deficient flies to infection, and points to a more prominent role for *BaraA* in antifungal defence.

280 ***IM10-like peptides display antifungal activity in vitro***

281

282 *The Baramicin A* gene encodes a polypeptide precursor that ultimately
283 produces multiple mature peptides. However the most prominent *BaraA* products
284 are the 23-residue IM10, 12, and 13 peptides (collectively the "IM10-like" peptides);
285 indeed three IM10-like peptides are produced for every one IM24 peptide (**Fig.** 2B),
286 and IM22 also bears an IM10-like motif (**Fig.** S3). This prompted us to explore the in
287 vitro activity of the BaraA IM10-like peptides as potential AMPs.

288

289 We synthesized IM10, IM12, and IM13 and performed in vitro antimicrobial
290 assays with these three IM10-like peptides using a 1:1:1 cocktail with a final
291 concentration of 300μM (100 μM each of IM10, IM12, and IM13). Using a protocol
292 adapted from Wiegand et al. [24], we monitored the microbicidal activity of this
293 peptide cocktail either alone, or in combination with membrane-disrupting
294 antibiotics that facilitate peptide entry into the cell. We based this approach on
295 previous studies that showed that the microbicidal activities of Abaecin-like
296 peptides, which target the bacterial DNA chaperone *DnaK,* increase exponentially in
297 combination with a membrane disrupting agent [25–27]. We did not detect any
298 killing activity of our IM10-like peptide cocktail alone against *Pectobacterium*
299 *carotovora Ecc15* (hereafter *"Ecc15"*), *Enterococcus faecalis,* or *C. albicans*. We also
300 found no activity of IM10-like peptides against *Ecc15 or E. faecalis* when co-
301 incubated with a sub-lethal dose of Cecropin or Ampicillin respectively. However,
302 we observed a synergistic interaction between IM10-like peptides and the
303 antifungal Pimaricin against *C. albicans* (**Fig.** 3D). Co-incubation of the IM10-like
304 cocktail with Pimaricin significantly improved the killing activity of Pimaricin at
305 32μg/mL relative to either treatment alone. While not statistically significant, the
306 combination of IM10-like cocktail and Pimaricin also outperformed either the IM10-
307 like cocktail alone or Pimaricin alone across the entire range of Pimaricin
308 concentrations tested.

309

310 We next co-incubated dilute preparations of *B. bassiana* strain R444 spores
311 under the same conditions as used previously with *C. albicans*, plated 2μL droplets,
312 and assessed the diameters and corresponding surface area of colonies derived from
313 individual spores after 4 days of growth at 25°C to assess growth rate. We found
314 that neither the IM10-like cocktail nor Pimaricin alone affected surface area relative
315 to PBS buffer control alone (Tukey's HSD: $p = 0.656$ and 0.466 respectively).
316 However in combination, the IM10-like cocktail plus Pimaricin led to significantly
317 reduced colony size compared to either treatment alone, corresponding to a 19-29%
318 reduction in surface area relative to controls (**Fig.** 3E, Tukey's HSD: $p < .01$ in all
319 cases). This indicates that incubation with IM10-like peptides and Pimaricin
320 synergistically inhibits *B. bassiana* mycelial growth, revealing an otherwise cryptic
321 antifungal effect of the BaraA IM10-like peptides.
322
323 Overall, we found that IM10-like peptides alone do not kill *C. albicans* yeast
324 or impair *B. bassiana* mycelial growth in vitro. However, IM10-like peptides seem to
325 synergize with the antifungal Pimaricin to inhibit growth of both of these fungi.
326
327 ***BaraA deficient flies broadly resist like wild type upon bacterial infection***
328
329 To further characterize *BaraA* function, we generated a null mutation of
330 *BaraA* by replacing the 'entire' *BaraA* locus with a dsRed cassette using CRISPR
331 mediated homology-directed repair with fly stocks that contain only one *BaraA* gene
332 copy (BL2057 and BL51323). After isolation, this mutation ($BaraA^{SW1}$) was then
333 backcrossed once to a lab strain of w^{1118} (used in [12–14]) to remove a second site
334 mutation (see materials and methods). The resulting w^{1118}; $BaraA^{SW1}$ flies are hereon
335 referred to as *"w; ΔBaraA*." Finally, the $BaraA^{SW1}$ mutation was isogenized by seven
336 rounds of backcrossing into the w^{1118} *DrosDel* isogenic genetic background (*iso*
337 w^{1118}) [28] as described in Ferreira et al and are hereon referred to as "*iso ΔBaraA*"
338 [29]. Relevant to this study, both our *OR-R* and *DrosDel iso* w^{1118} wild type lines
339 contain the duplication and thus have both *BaraA1 and A2* genes, while *w; ΔBaraA*

340 and *iso ΔBaraA* flies lack *BaraA* entirely. In the following experiments, we compare
341 the immune response of both *w; ΔBaraA* and *iso ΔBaraA* and focused only on
342 phenotypes that were consistent in both genetic backgrounds.
343
344 We validated these mutant lines by PCR, qPCR and MALDI-TOF peptidomics
345 (**Fig.** 2A, supplementary data file 1). *BaraA*-deficient flies were viable with no
346 morphological defect. Furthermore, *ΔBaraA* flies have wild type Toll and Imd
347 signalling responses following infection, indicating that *BaraA* is not required for the
348 activation of these signaling cascades (**Fig.** S5A-C). Moreover, *BaraA* mutant flies
349 survive clean injury like wild type (**Fig.** S5D), and have comparable lifespan to wild
350 type flies (**Fig.** S5E). We next challenged *BaraA* mutant flies using our two genetic
351 backgrounds with a variety of pathogens. We included susceptible Imd deficient
352 Rel^{E20} flies, Toll deficient spz^{rm7} flies and *Bomanin* deficient $Bom^{\Delta 55C}$ flies as
353 comparative controls. We observed that *BaraA* null flies have comparable resistance
354 as wild type to infection with the Gram-negative bacterium *Ecc15* (**Fig.** S6A), or with
355 the Gram-positive bacterium *B. subtilis* (**Fig.** S6B). In contrast, we saw a mild
356 increase in the susceptibility of *w; ΔBaraA* flies to infection by the Gram-positive
357 bacterium *E. faecalis* (HR = +0.73, p = .014). We also saw an early mortality
358 phenotype in *iso ΔBaraA* flies (at 3.5 days, p < .001), although this was not ultimately
359 statistically significant (**Fig.** 4A; p = .173). This mild susceptibility was also observed
360 using flies carrying the *BaraA* mutation over a deficiency (*ΔBaraA/Df(BaraA))*, as
361 well as in flies ubiquitously expressing *BaraA* RNAi (**Fig.** S7); however none of these
362 sets of survival experiments individually reached statistical significance. Overall, the
363 susceptibility of *BaraA* mutants to *E. faecalis* is mild, but consistent using a variety of
364 genetic approaches.

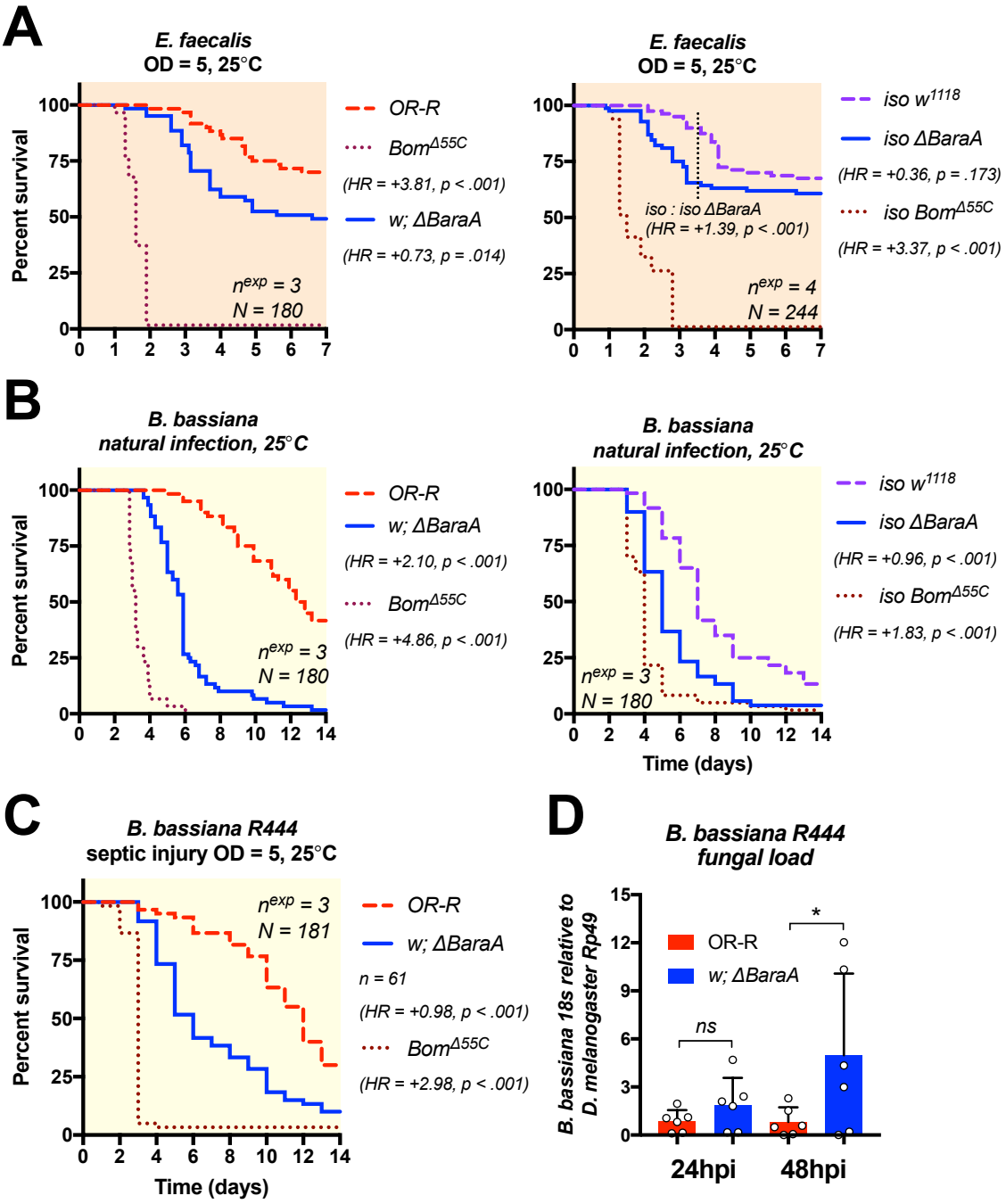

Figure 4: *ΔBaraA* flies are most susceptible to fungal infection. A) *BaraA* mutants with two different genetic backgrounds (here called *w* or *iso*) display a mild susceptibility to systemic infection with *E. faecalis*. This presents as an earlier mortality in the *iso* background (dotted line, p < .001). However, survival in *iso ΔBaraA* flies was not significantly different from wild type at seven days post-infection (p = .173). B) *BaraA* mutants in both backgrounds are susceptible to natural infection with the entomopathogenic fungus *B. bassiana*. C-D) Increased susceptibility (C) and fungal load (D) of *ΔBaraA* flies upon systemic infection by *B. bassiana strain R444*.

374 ***BaraA mutant flies are highly susceptible to Beauveria fungal infection***

375

376 Entomopathogenic fungi such as *B. bassiana* represent an important class of
377 insect pathogens [6]. They have the ability to directly invade the body cavity by
378 digesting and crossing through the insect cuticle. The Toll pathway is critical to
379 survive fungal pathogens as it is directly responsible for the expression of *Bomanin*,
380 *Daisho*, *Drosomycin* and *Metchnikowin* antifungal effectors [12,14,15,30,31]. The fact
381 that i) *BaraA* is Toll-regulated, ii) BaraA IM10-like peptides display antifungal
382 activity in vitro, and iii) *BaraA* overexpression improves the resistance of *Imd, Toll*
383 deficient flies against fungi all point to a role for *BaraA* against fungal pathogens.

384

385 We infected *BaraA* mutants and wild type flies by rolling flies in sporulating
386 *B. bassiana* petri dishes. Strikingly, both *w; ΔBaraA* and *iso ΔBaraA* flies displayed a
387 pronounced susceptibility to natural infection with *B. bassiana* (HR = +2.10 or +0.96
388 respectively, $p < .001$ for both) (**Fig.** 4B). An increased susceptibility to fungi was
389 also observed using flies carrying the *BaraA* mutation over a deficiency (**Fig.** S8A) or
390 that ubiquitously express *BaraA* RNAi (**Fig.** S8B). Moreover, constitutive *BaraA*
391 expression (*Act-Gal4>UAS-BaraA)* in an otherwise wild type background improves
392 survival to *B. bassiana* relative to *Act-Gal4>OR-R* controls (HR = -0.52, $p = .010$) (**Fig.**
393 S8C). Finally, we used a preparation of commercial *B. bassiana R444* spores (BB-
394 PROTEC, Andermatt Biocontrol) to perform controlled systemic infections by
395 pricking flies with a needle dipped in spore solution. In these experiments we
396 monitored both survival and fungal load using qPCR primers specific to the *B.*
397 *bassiana* 18S rRNA gene [32]. As seen with natural infection, *BaraA* mutants were
398 highly susceptible to *Beauveria* systemic infection (**Fig.** 4C). Moreover, *BaraA*
399 mutants suffered increased fungal load by 48 hours after infection (**Fig.** 4D).

400

401 Collectively, our survival analyses point to an important role for *BaraA* in
402 defence against the entomopathogenic fungus *B. bassiana*. Consistent with a direct
403 effect of *BaraA* on fungi, we observe a susceptibility of *BaraA* mutants to infection
404 that is correlated with increased proliferation of *B. bassiana*.

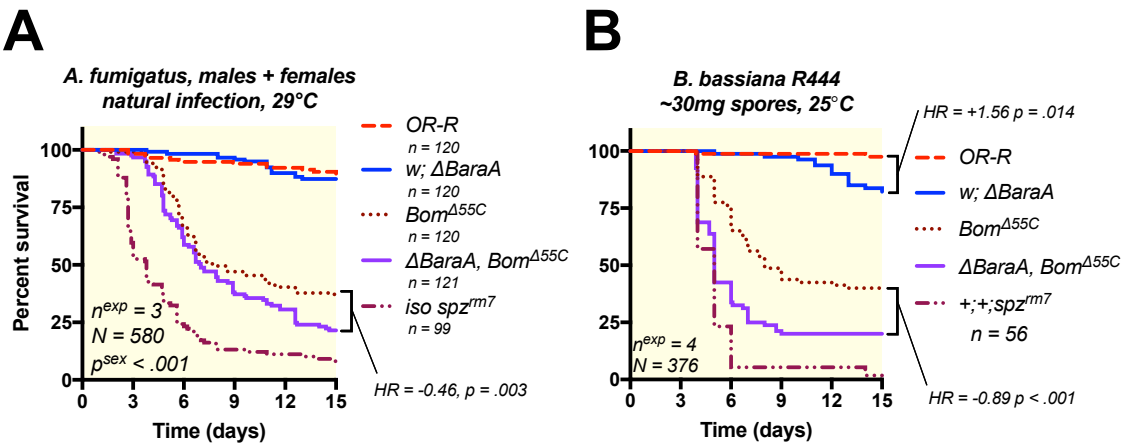

Figure 5: *BaraA* contributes to antifungal defence independent of *Bomanins*. A) *ΔBaraA* , *Bom*$^{\Delta 55C}$ double mutant flies were more susceptible than either mutation alone to natural infection with *A. fumigatus* (see Fig. S6C-D for sex-specific survival curves). B) *ΔBaraA* , *Bom*$^{\Delta 55C}$ double mutant flies were similarly more susceptible than individual mutants when given a mild (30mg of spores) *Beauveria* natural infection by *B. bassiana R444.*

BaraA contributes to antifungal defence independent of Bomanins

Use of compound mutants carrying multiple mutations in effector genes has shown that some of them additively contribute to host resistance to infection [15]. Compound deletions of immune genes can also reveal contributions of immune effectors that are not detectable via single mutant analysis [15,33,34]. Recent studies have indicated that *Bomanins* play a major role in defence against fungi [12,13], though their mechanism of action is unknown. It is possible that *Bomanin* activity relies on the presence of *BaraA*, or vice versa. This prompted us to investigate the interaction of *Bomanins* and *BaraA* in defence against fungi. To do this, we recombined the *Bom*$^{\Delta 55C}$ mutation (that removes a cluster of 10 *Bomanin* genes) with *ΔBaraA.* While natural infection with *Aspergillus fumigatus* did not induce significant mortality in *BaraA* single mutants (**Fig.** S6C-D), we observed that combining *ΔBaraA* and *Bom*$^{\Delta 55C}$ mutations increases fly susceptibility to this pathogen relative to *Bom*$^{\Delta 55C}$ alone (HR = -0.46, p = .003; **Fig.** 5A). We next exposed these *ΔBaraA*, *Bom*$^{\Delta 55C}$, double mutant flies to natural infection with 30mg of commercial spores of *B. bassiana R444*, which we found to be a less virulent *Beauveria* infection model. This is equivalent to approximately 60 million spores,

430 much of which are removed afterwards upon fly grooming. When using this
431 infection method, we found that *BaraA* mutation markedly increases the
432 susceptibility of $Bom^{\Delta 55C}$ mutant flies (HR = -0.89, $p < .001$), approaching spz^{rm7}
433 susceptibility (**Fig.** 5B).
434
435 We conclude that the contribution of *BaraA* to defence does not rely on the
436 presence of *Bomanins*, and vice versa. This finding is consistent with the ability of
437 constitutively expressed *BaraA* to improve survival outcome even in *Imd, Toll*
438 deficient flies. Taken together, these results suggest *BaraA* improves survival
439 against fungi independent of other effectors of the systemic immune response,
440 consistent with a direct effect on invading fungi.
441
442 ***ΔBaraA males display an erect wing phenotype upon infection***
443
444 While performing infections with *A. fumigatus*, we observed a high
445 prevalence of *BaraA* mutant flies with upright wings (**Fig.** 6A-B), a phenotype
446 similar to the effect of disrupting the gene encoding the "*erect wing"* (*ewg*)
447 transcription factor [35]. Curiously, this erect wing phenotype was most specifically
448 observed in males. Upon further observation, erect wing was observed not only
449 upon *A. fumigatus* infection, but also upon infections with all Gram-positive bacteria
450 and fungi tested (**Table** S1). Increased prevalence of erect wing flies was observed
451 upon infection with both live (**Fig.** 6C) and heat-killed *E. faecalis* (**Fig.** 6D), but less
452 so upon clean injury or via infection with the Gram-negative bacteria *Ecc15* (**Fig.**
453 S9A-B). Thus, the erect wing phenotype appears to be observed in *BaraA* mutants in
454 response to stimuli known to activate the Toll pathway, but does not require a live
455 infection.
456
457 Such a phenotype in infected males has never been reported, but is
458 reminiscent of the wing extension behaviour of flies infected by the brain-
459 controlling "zombie" fungus *Enthomopthera muscae* [36]. Intrigued by this
460 phenotype, we further explored its prevalence in other genetic backgrounds. We

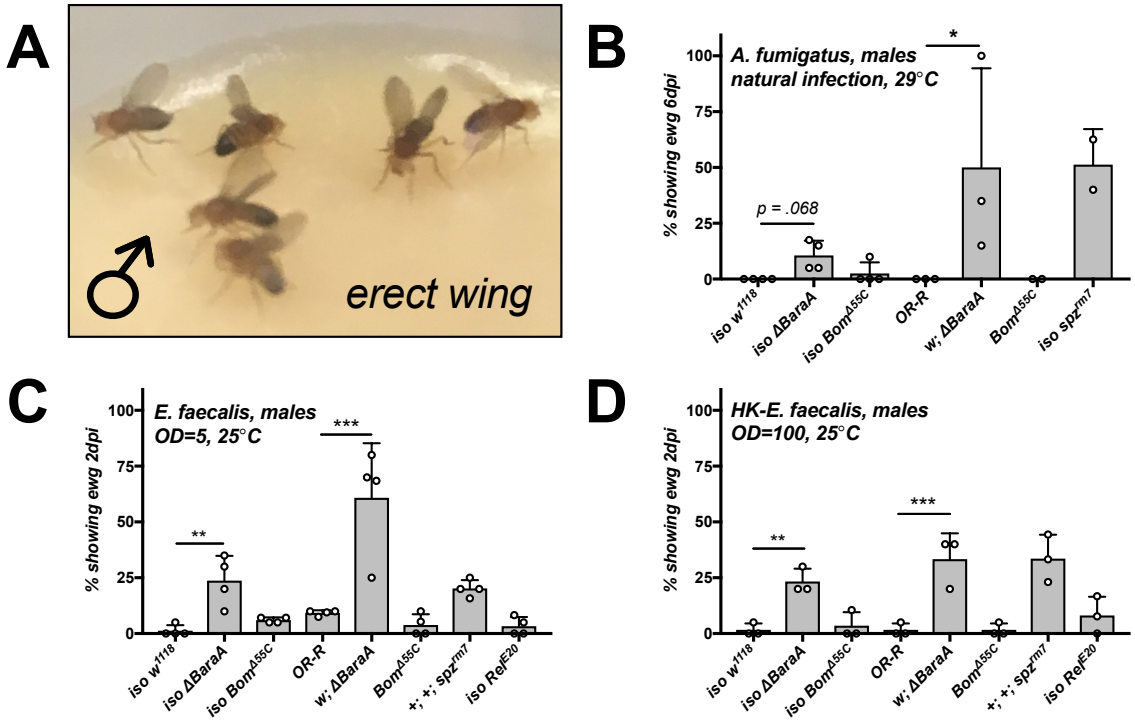

Figure 6: *ΔBaraA* males display an erect wing phenotype upon infection. A) *ΔBaraA* males displaying erect wing six days after *A. fumigatus* natural infection. B-D) *spz*^{rm7} and *ΔBaraA* males, but not *Bom*$^{\Delta 55C}$ or *Rel*^{E20} flies display the erect wing phenotype upon natural infection with *A. fumigatus* (B), or septic injury with live (C) or heat-killed *E. faecalis* (D). Barplots show the percentage of flies displaying erect wing following treatment, with individual data points reflecting replicate experiments. Additional challenges are shown in Table S1.

next confirmed that this phenotype was also observed in other *BaraA*-deficient backgrounds such as *Df(BaraA)/ΔBara*; however the penetrance was variable from one background to another. Erect wing was also observed in *ΔBaraA*/+ heterozygous flies (*Df(BaraA)/+* or *ΔBaraA*/+), indicating that the lack of *BaraA* on one chromosome was sufficient to cause the phenotype (**Fig.** S9C and **Table** S1). Moreover, *spz*^{rm7} flies that lack functional Toll signalling phenocopy *ΔBaraA* flies and display erect wing, but other immune-deficient genotypes such as mutants for the Toll-regulated *Bomanin* effectors (*Bom*$^{\Delta 55C}$), or *Rel*^{E20} mutants that lack Imd signalling, did not readily display erect wing (**Fig.** 6C-D, **Table** S1). Thus the erect wing phenotype is not linked to susceptibility to infection, but rather to loss of *BaraA* upon stimuli triggering the Toll immune pathway. This phenotype suggests

480 an additional effect of *BaraA* on tissues related to the wing muscle or in the nervous
481 system.
482

483 # Discussion:

484

485 Seven *Drosophila* AMP families were identified in the 1980s-1990s either by
486 homology with AMPs characterized in other insects or owing to their abundant
487 production and microbicidal activities in vitro [37]. In the 2000s, genome
488 annotations revealed the existence of many additional paralogous genes from the
489 seven well-defined families of AMPs [38,39]. At that time, microarray and MALDI-
490 TOF analyses also revealed the existence of many more small immune-induced
491 peptides, which may function as AMPs [8,22]. Genetic analyses using loss of function
492 mutations have recently shown that some of these peptides do play an important
493 role in host defence, however key points surrounding their direct microbicidal
494 activities remain unclear. In 2015, *Bomanins* were shown to be critical to host
495 defence using genetic approaches, but to date no activity in vitro has been found
496 [12,13]. Two candidate AMPs, Listericin [40] and GNBP-like3 [41], were shown to
497 inhibit microbial growth upon heterologous expression using S2 cell lines or
498 bacteria respectively. Most recently, Daisho peptides were shown to bind to fungal
499 hyphae ex vivo, and are required for resisting fungal infection in vivo [14]. However
500 the mechanism and direct microbicidal activity of these various peptides at
501 physiological concentrations was not assessed.
502

503 In this study, we provide evidence from four separate experimental
504 approaches that support adding *BaraA* to the list of bona-fide antifungal peptides.
505 First, the *BaraA* gene is strongly induced in the fat body upon infection resulting in
506 abundant peptide production. *BaraA* is also tightly regulated by the Toll pathway,
507 which orchestrates the antifungal response. Second, loss of function study shows
508 that *BaraA* contributes to resistance against fungi. *BaraA* mutation increases
509 susceptibility to *B. bassiana*, and this is coupled with increased *B. bassiana*

510 proliferation. Third, the antifungal activity of *BaraA* is independent of other key
511 effectors. Over-expression of *BaraA* in the absence of other inducible peptides
512 increased resistance of *Imd, Toll* deficient flies to various fungi including *C. albicans*,
513 *A. fumigatus*, and *N. crassa*. Moreover *BaraA, Bomanin* double mutants suffered
514 greater susceptibility than *Bomanin* mutants alone upon natural infection, even with
515 a relatively avirulent fungal pathogen (*A. fumigatus*). Fourth, and lastly, a cocktail of
516 the *BaraA* IM10-like peptides possesses antifungal activity against *C. albicans* and *B.*
517 *bassiana* in vitro when co-incubated with the membrane disrupting antifungal
518 Pimaricin.
519
520 While it is difficult to estimate the concentration of BaraA peptides in the
521 haemolymph of infected flies, it is expected based on MALDI-TOF peak intensities
522 that the IM10-like peptides should reach concentrations similar to other AMPs (up
523 to 100μM) [10,20]; our in vitro assays used a peptide cocktail at the upper limit of
524 this range. AMPs are often - but not exclusively – positively charged. This positive
525 charge is thought to recruit these molecules to negatively charged membranes of
526 microbes [10]. However the net charges at pH=7 of the IM10-like peptides are: IM10
527 +1.1, IM12 +0.1, and IM13 -0.9. Given this range of net charge, IM10-like peptides
528 are not overtly cationic. However some AMPs are antimicrobial without being
529 positively charged, exemplified by human Dermicidin [42] and anionic peptides of
530 Lepidoptera that also synergize with membrane-disrupting agents [43]. More
531 extensive in vitro experiments with additional fungi should confirm the range of
532 BaraA peptide activities, and assay the potential activities of IM22 and IM24, which
533 were not included in this study.
534
535 Our study also reveals that the *Baramicin A* gene alone produces at least 1/3
536 of the initially reported IMs. In addition to the IM10-like peptides and IM24 that
537 were previously assigned to *BaraA* [22], we show IM22 is encoded by the C terminus
538 of *BaraA*, and is conserved in other *Drosophila* species. The production of multiple
539 IMs encoded as tandem repeats between furin cleavage sites is built-in to the BaraA
540 protein design akin to a "protein operon." Such tandem repeat organization is rare,

541 but not totally unique among AMPs. This structure was first described in the
542 bumblebee AMP Apidaecin [44], and has since also been found in Drosocin of
543 *Drosophila neotestacea* [45]. In *D. melanogaster*, several AMPs are furin-processed
544 including Attacin C and its pro-peptide MPAC, wherein both parts synergize in
545 killing bacteria [25]. Therefore, furin cleavage in Attacin C enables the precise co-
546 expression of distinct peptides with synergistic activity. It is interesting to note that
547 IM10-like peptides did not show antifungal activity in the absence of membrane
548 disruption by Pimaricin. An attractive hypothesis is that longer peptides encoded by
549 BaraA such as IM22 and IM24 could contribute to the antifungal activity of *BaraA* by
550 membrane permeabilization, allowing the internalization of IM10-like peptides.
551 Indeed, the BaraA IM24 peptide is a short Glycine-rich peptide (96 AA) that is
552 positively-charged (charge +2.4 at pH=7). These traits are shared by amphipathic
553 membrane-disrupting AMPs such as Attacins [10], however the precise role for the
554 Baramicin IM24 domain remains to be determined.
555
556 An unexpected observation of our study is the display of an erect wing
557 phenotype by *BaraA* deficient males upon infection. Our study suggests that this is
558 not a consequence of the genetic background, but rather relies on the activation of
559 the Toll pathway in the absence of *BaraA*. Erect wing is also induced by heat-killed
560 bacteria, and is not observed in *Bomanin* or *Relish* mutants, indicating that the erect
561 wing phenotype is not a generic consequence of susceptibility to infection. The *erect*
562 *wing* gene, whose inactivation causes a similar phenotype, is a transcription factor
563 that regulates synaptic growth in developing neuromuscular junctions [35]. This
564 raises the intriguing hypothesis that immune processes downstream of the Toll
565 ligand Spaetzle somehow affect wing neuromuscular junctions, and that *BaraA*
566 modulates this activity. Another puzzling observation is the sexual dimorphism
567 exhibited for this response. Male courtship and aggression displays involve similar
568 wing extension behaviours. Koganezawa et al. [46] showed that males deficient for
569 *Gustatory receptor 32a (Gr32a)* failed to unilaterally extend wings during courtship
570 display. *Gr32a*-expressing cells extend into the subesophageal ganglion where they
571 contact mAL, a male-specific set of interneurons involved in unilateral wing display

572 [46]. One possible explanation for the male specific effects of BaraA could be that
573 *BaraA* mediates this effect through interactions with such male-specific neurons.
574 *BaraA* is highly produced in the fat body upon infection but also expressed in the
575 nervous system (**Fig.** 1D-E and FlyAtlas1 [21]). Further studies should decipher
576 whether the preventative effect of *BaraA* on the erect wing phenotype is cell
577 autonomous or linked to BaraA peptides secreted into the haemolymph. Recent
578 studies have highlighted how NF-κB signalling in the brain is activated by bacterial
579 peptidoglycan [47], and that immune effectors expressed either by fat body
580 surrounding the brain or from within brain tissue itself affect memory formation
581 [41]. Moreover, an AMP of nematodes regulates aging-dependent
582 neurodegeneration through binding to its G-protein coupled receptor, and this
583 pathway is sufficient to trigger neurodegeneration following infection [48]. Thus
584 immune-inducible AMPs can have striking interactions with neurological processes.
585 As such, future studies characterizing the role of *BaraA* in the erect wing phenotype
586 should provide insight on interactions between systemic immunity and host
587 physiology more generally.
588
589 Here we describe a complex immune effector gene that produces multiple
590 peptide products. *BaraA* encodes many of the most abundant immune effectors
591 induced downstream of the Toll signalling pathway, and indeed *BaraA* promotes
592 survival upon fungal infection. How each peptide contributes to the immune
593 response and/or erect wing behaviour will be informative in understanding the
594 range of effects immune effectors can have on host physiology. This work and others
595 also clarifies how the cocktail of immune effectors produced upon infection acts
596 specifically during innate host defence reactions.

597 # Materials and methods:

598

599 *Fly genetics and sequence comparisons*

600

601 Sequence files were collected from FlyBase [49] and recently-generated
602 sequence data [45,50] and comparisons were made using Geneious R10. Putative
603 NF-κB binding sites were annotated using the Relish motif "GGRDNNHHBS"
604 described in Copley et al. [18] and a manually curated amalgam motif of
605 "GGGHHNNDVH" derived from common Dif binding sites described previously
606 [17,19]. Gene expression analyses were performed using primers described in
607 supplementary data file 1, and further microarray validation for *BaraA* expression
608 comes from De Gregorio et al. [11].

609

610 The *UAS-BaraA* and *BaraA-Gal4* constructs were generated using the TOPO
611 pENTR entry vector and cloned into the pTW or pBPGUw Gateway™ vector systems
612 respectively. The *BaraA-Gal4* promoter contains 1675bp upstream of *BaraA1* (but
613 also *BaraA2,* sequence in supplementary information). The *BaraA-Gal4* construct
614 was inserted into the VK33 attP docking site (BDSC line #24871). The $BaraA^{SW1}$
615 (*ΔBaraA)* mutant was generated using CRISPR with two gRNAs and an HDR vector
616 by cloning 5' and 3' region-homologous arms into the pHD-dsRed vector, and
617 consequently *ΔBaraA* flies express dsRed in their eyes, ocelli, and abdomen. *ΔBaraA*
618 was generated using the Bloomington stocks BL2057 and BL51323 as these
619 backgrounds contain only one copy of the *BaraA* locus. The induction of the immune
620 response in these flies was validated by qPCR and MALDI-TOF proteomics, wherein
621 we discovered an aberrant *Dso2* locus in these preliminary $BaraA^{SW1}$ flies. We thus
622 backcrossed the $BaraA^{SW1}$ mutation once with a standard w^{1118} background (used in
623 [12–14]) and screened for wild type *Dso2* before use in any survival experiments.
624 Additionally, *ΔBaraA* was isogenized into the *DrosDel* w^{1118} isogenic background for
625 seven generations before use in isogenic fly experiments as described in Ferreira et
626 al. [29].

627
628 A full description of fly stocks used for crosses and in experiments is provided in
629 supplementary data file 1.
630
631 *Microbe culturing conditions*
632
633 Bacteria and *C. albicans* yeast were grown to mid-log phase shaking at
634 200rpm in their respective growth media (Luria Bertani, Brain Heart Infusion, or
635 Yeast extract-Peptone-Glycerol) and temperature conditions, and then pelleted by
636 centrifugation to concentrate microbes. Resulting cultures were diluted to the
637 desired optical density at 600nm (OD) for survival experiments, which is indicated
638 in each figure. The following microbes were grown at 37°C: *Escherichia coli strain*
639 *1106* (LB), *Enterococcus faecalis* (BHI), and *Candida albicans* (YPG). The following
640 microbes were grown at 29°C: *Erwinia carotovora carotovora (Ecc15)* (LB) and
641 *Micrococcus luteus* (LB). For filamentous fungi and molds, *Aspergillus fumigatus* was
642 grown at 37°C, and *Neurospora crassa* and *Beauveria bassiana* were grown at room
643 temperature on Malt Agar in the dark until sporulation. *Beauveria bassiana strain*
644 *R444* commercial spores were produced by Andermatt Biocontrol, product: BB-
645 PROTEC.
646
647 *Survival experiments*
648
649 Survival experiments were performed as previously described [15], with 20
650 flies per vial with 2-3 replicate experiments. 3-5 day old males were used in
651 experiments unless otherwise specified. As *Rel, spz* double mutant flies and largely
652 wild type backgrounds differ drastically in their immune competence, we selected
653 pathogens, infection routes, and temperatures to provide infection models that
654 could best reveal phenotypes in these disparate genetic backgrounds. For fungi
655 natural infections, flies were flipped at the end of the first day to remove excess
656 fungal spores from the vials. Otherwise, flies were flipped thrice weekly. Statistical

657 analyses were performed using a Cox proportional hazards (CoxPH) model in R
658 3.6.3. We report the hazard ratio (HR) alongside p-values as a proxy for effect size in
659 survival experiments. Throughout our analyses, we required $p < .05$ as evidence to
660 report an effect as significant, but note interactions with |HR| near or above 0.5 as
661 potentially important provided p-value approached .05, and tamp down importance
662 of interactions that were significant, but have relatively minor effect size (|HR| less
663 than 0.5) in our discussion of the data.
664
665 *Erect wing scoring*
666
667 The erect wing phenotype was scored as the number of flies with splayed
668 wings throughout a distinct majority of the period of observation (30s); if unclear,
669 the vial was monitored an additional 30s. Here we define splayed wings as wings
670 not at rest over the back, but did not require wings to be fully upright; on occasion
671 wings were held splayed outward at ~45° relative to the dorsal view, and often
672 slightly elevated relative to the resting state akin to male aggressive displays.
673 Sometimes only one wing was extended, which occurred in both thoracic pricking
674 and fungi natural infections; these flies were counted as having erect wing. In
675 natural infections, the typical course of erect wing display developed in two fashions
676 at early time points, either: i) flies beginning with wings slightly splayed but not
677 fully upright, or ii) flies constantly flitting their wings outward and returning them
678 to rest briefly, only to flit them outward again for extended periods of time. Shortly
679 after infection, some flies were also observed wandering around with wings beating
680 at a furious pace, which was not counted as erect wing. However at later time points
681 erect wing flies settled more permanently on upright splayed wings. Erect wing
682 measurements were taken daily following infection, and erect wing flies over total
683 flies was converted to a percent. Data points in **Fig.** 6B-D represent % with erect
684 wing in individual replicate experiments with ~20 flies per vial. Flies stuck in the
685 vial, or where the wings had become sticky or mangled were not included in totals.
686 **Table** S1 reports mean percentages across replicate experiments for all pathogens

687 and genotypes where erect wing was monitored. Days post-infection reported in
688 **Table** S1 were selected as the final day prior to major incidents of mortality. For *E.*
689 *faecalis* live infections, *Bom*$^{\Delta 55C}$ and *spz*^{rm7} erect wing was taken at 1dpi due to major
690 mortality events by 2dpi specifically in these lines.
691
692 Erect wing measurements were performed in parallel with survival
693 experiments, which often introduced injury to the thorax below the wing possibly
694 damaging flight muscle. It is unlikely that muscle damage explains differences in
695 erect wing display. First: we noticed erect wing initially during natural infections
696 with *A. fumigatus*, and observed erect wing upon *B. bassiana R444* and *Metarhizium*
697 *rileyi PHP1705* natural infections (**Table** S1; *M. rileyi* = NOMU-PROTEC, Andermatt
698 Biocontrol). Second: only 1 of 75 total *iso w*^{1118} males displayed erect wing across 4
699 systemic infection experiments with *E. faecalis*. For comparison: 19 of 80 total *iso*
700 *ΔBaraA* and 48 of 80 *w; ΔBaraA* flies displayed erect wing (**Table** S1). Future studies
701 might be better served using an abdominal infection mode, which can have different
702 infection dynamics [51]. However we find erect wing display to be robust upon
703 either septic injury or natural infection modes.
704
705 *IM10-like peptide in vitro activity*
706
707 The 23-residue Baramicin peptides were synthesized by GenicBio to a purity
708 of >95%, verified by HPLC. An N-terminal pyroglutamate modification was included
709 based on previous peptidomic descriptions of Baramicins IM10, IM12, and IM13
710 [52], which we also detected in our LC-MS data (**Fig.** S2). Peptides were dissolved in
711 DMSO and diluted to a working stock of 1200μM in 0.6% DMSO; the final
712 concentration for incubations was 300μM in 0.15% DMSO. For microbe-killing
713 assays, microbes were allowed to grow to log-growth phase, at which point they
714 were diluted to ~50cells/μL. Two μL of culture (~100 cells), and 1μL water or
715 antibiotic was mixed with 1μL of a 1:1:1 cocktail of IM10, IM12, and IM13 peptides
716 to a final concentration of 300μM total peptides; 1μL of water + DMSO (final
717 concentration = 0.15% DMSO) was used as a negative control. Four μL microbe-

718 peptide solutions were incubated for 24h at 4°C. Microbe-peptide cultures were
719 then diluted to a final volume of 100μL and the entire solution was plated on LB
720 agar or BiGGY agar plates. Colonies were counted manually. For combinatorial
721 assays with bacteria, *C. albicans* yeast, and *B. bassiana R444* spores, peptide cocktails
722 were combined with membrane disrupting antimicrobials effective against relevant
723 pathogens beginning at: 10 μM Cecropin A (Sigma), 500μg/mL ampicillin, or
724 250μg/mL Pimaricin (commercially available as "Fungin," InVivogen), serially
725 diluted through to 0.1 μM, 0.5μg/mL, and 4μg/mL respectively.
726
727 *Beauveria bassiana R444* spores were prepared by dissolving ~30mg of
728 spores in 10mL PBS, and then 4μL microbe-peptide solutions were prepared as
729 described for *C. albicans* followed by incubation for 24h at 4°C; this spore density
730 was optimal in our hands to produce distinct individual colonies. Then, 4μL PBS was
731 added to each solution and 2μL droplets were plated on malt agar at 25°C. Colony
732 diameters were measured 4 days after plating by manually analyzing colony
733 diameters in InkScape v0.92. Experimental batches were included as co-variates in
734 one-way ANOVA analysis. The initial dataset approached violating Shapiro-Wilk
735 assumptions of normality ($p = 0.061$) implemented in R 3.6.3. We subsequently
736 removed four colonies from the analysis, as these outliers were over two standard
737 deviations lower than their respective mean (removed colonies: PBS 0.15cm, PBS
738 0.25cm, IM10-like+Pimaricin 0.21cm, and a second IM10-like+Pimaricin colony of
739 0.21cm); the resulting Shapiro-Wilk p-value = 0.294, and both QQ and residual plots
740 suggested a normal distribution. Final killing activities and colony surface areas
741 were compared by One-way ANOVA with Holm-Sidak multiple test correction (*C.*
742 *albicans*) and Tukey's honest significant difference multiple test correction (*B.*
743 *bassiana R444*).
744
745
746
747

748 *Gene expression analyses*

749

750 RNA was extracted using TRIzol according to manufacturer's protocol. cDNA
751 was reverse transcribed using Takara Reverse Transcriptase. qPCR was performed
752 using PowerUP mastermix from Applied Biosystems at 60°C using primers listed in
753 supplementary data file 1. Gene expression was quantified using the PFAFFL
754 method [53] with *Rp49* as the reference gene. Statistical analysis was performed by
755 one-way ANOVA with Holm-Sidak's multiple test correction or student's t-test. Error
756 bars represent one standard deviation from the mean.

757

758 *Proteomic analyses*

759

760 Raw haemolymph samples were collected from immune-challenged flies for
761 MALDI-TOF proteomic analysis as described in [14,15]. MALDI-TOF proteomic
762 signals were confirmed independently at facilities in both San Diego, USA and
763 Lausanne, CH. In brief, haemolymph was collected by capillary and transferred to
764 0.1% TFA before addition to acetonitrile universal matrix. Representative spectra
765 are shown. Peaks were identified via corresponding m/z values from previous
766 studies [8,22]. Spectra were visualized using mMass, and figures were additionally
767 prepared using Inkscape v0.92.

768

769 **Author contributions:**

770

771 MAH planned experiments, performed bioinformatic analyses, infection
772 experiments, and in vitro assays. BL supervised the project and MAH and BL wrote
773 the manuscript. LC planned and generated the *BaraA* deletion and performed key
774 descriptive experiments and observations. AM assisted with infection and in vitro
775 assays. MH, II, and SAW generated and supplied critical fly stock reagents and
776 provided constructive commentary.

777

Acknowledgements:

This research was supported by Sinergia grant CRSII5_186397 and Novartis Foundation 532114 awarded to Bruno Lemaitre, and by National Institute of Health (NIH) grant R01 GM050545 to Steven Wasserman. We thank Jean-Philippe Boquete for assistance with the generation of Gal4 and UAS constructs. We would also like to acknowledge the technical expertise provided by the proteomics and mass spectrometry facilities in both UCSD and EPFL, and specifically Adrien Schmid. The name "*Baramicin*" was partly inspired by Eichero Oda's character "Buggy," a Bara-Bara superhuman. Finally, we further thank Huang et al. (*in preparation*) for their cooperation in publishing initial descriptions of the *BaraA* gene, and for stimulating discussion.

790 **References:**

791

792 1. Lemaitre B, Hoffmann J. The Host Defense of Drosophila Melanogaster. Annual
793 Review of Immunology. 2007;25: 697–743.
794 doi:10.1146/annurev.immunol.25.022106.141615

795 2. Kurz CL, Ewbank JJ. Caenorhabditis elegans: An emerging genetic model for the
796 study of innate immunity. Nature Reviews Genetics. 2003;4: 380–390.
797 doi:10.1038/nrg1067

798 3. Kaufmann SHE. Immunology's foundation: the 100-year anniversary of the
799 Nobel Prize to Paul Ehrlich and Elie Metchnikoff. Nat Immunol. 2008;9: 705–
800 712. doi:10.1038/ni0708-705

801 4. Steiner H, Hultmark D, Engström \AA, Bennich H, Boman HG. Sequence and
802 specificity of two antibacterial proteins involved in insect immunity. Nature.
803 1981;292: 246–248. doi:10.1038/292246a0

804 5. Lemaitre B, Nicolas E, Michaut L, Reichhart JM, Hoffmann JA. The dorsoventral
805 regulatory gene cassette spatzle/Toll/Cactus controls the potent antifungal
806 response in Drosophila adults. Cell. 1996;86: 973–983. doi:10.1016/S0092-
807 8674(00)80172-5

808 6. Lemaitre B, Reichhart JM, Hoffmann JA. Drosophila host defense: differential
809 induction of antimicrobial peptide genes after infection by various classes of
810 microorganisms. Proceedings of the National Academy of Sciences of the United
811 States of America. 1997;94: 14614–9. doi:10.1073/pnas.94.26.14614

812 7. Lemaitre B, Kromer-Metzger E, Michaut L, Nicolas E, Meister M, Georgel P, et al.
813 A recessive mutation, immune deficiency (imd), defines two distinct control
814 pathways in the Drosophila host defense. Proc Natl Acad Sci U S A. 1995;92:
815 9465–9469. doi:10.1073/pnas.92.21.9465

816 8. Uttenweiler-Joseph S, Moniatte M, Lagueux M, Van Dorsselaer a, Hoffmann J a,
817 Bulet P. Differential display of peptides induced during the immune response of
818 Drosophila: a matrix-assisted laser desorption ionization time-of-flight mass
819 spectrometry study. Proceedings of the National Academy of Sciences of the
820 United States of America. 1998;95: 11342–11347.
821 doi:10.1073/pnas.95.19.11342

822 9. Lazzaro BP, Zasloff M, Rolff J. Antimicrobial peptides: Application informed by
823 evolution. Science. 2020;368. doi:10.1126/science.aau5480

824 10. Hanson MA, Lemaitre B. New insights on Drosophila antimicrobial peptide
825 function in host defense and beyond. Curr Opin Immunol. 2020;62: 22–30.
826 doi:10.1016/j.coi.2019.11.008

827 11. De Gregorio E, Spellman PT, Tzou P, Rubin GM, Lemaitre B. The Toll and Imd
828 pathways are the major regulators of the immune response in Drosophila.
829 EMBO Journal. 2002;21: 2568–2579. doi:10.1093/emboj/21.11.2568

830 12. Clemmons AW, Lindsay SA, Wasserman SA. An Effector Peptide Family
831 Required for Drosophila Toll-Mediated Immunity. PLoS Pathogens. 2015;11.
832 doi:10.1371/journal.ppat.1004876

833 13. Lindsay SA, Lin SJH, Wasserman SA. Short-Form Bomanins Mediate Humoral
834 Immunity in Drosophila. J Innate Immun. 2018;10: 306–314.
835 doi:10.1159/000489831

836 14. Cohen LB, Lindsay SA, Xu Y, Lin SJH, Wasserman SA. The Daisho Peptides
837 Mediate Drosophila Defense Against a Subset of Filamentous Fungi. Front
838 Immunol. 2020;11: 9. doi:10.3389/fimmu.2020.00009

839 15. Hanson MA, Dostálová A, Ceroni C, Poidevin M, Kondo S, Lemaitre B. Synergy
840 and remarkable specificity of antimicrobial peptides in vivo using a systematic
841 knockout approach. eLife. 2019;8. doi:10.7554/elife.44341

842 16. Unckless RL, Howick VM, Lazzaro BP. Convergent Balancing Selection on an
843 Antimicrobial Peptide in Drosophila. Current Biology. 2016;26: 257–262.
844 doi:10.1016/j.cub.2015.11.063

845 17. Busse MS, Arnold CP, Towb P, Katrivesis J, Wasserman SA. A κB sequence code
846 for pathway-specific innate immune responses. EMBO Journal. 2007;26: 3826–
847 3835. doi:10.1038/sj.emboj.7601798

848 18. Copley RR, Totrov M, Linnell J, Field S, Ragoussis J, Udalova IA. Functional
849 conservation of Rel binding sites in drosophilid genomes. Genome Research.
850 2007;17: 1327–1335. doi:10.1101/gr.6490707

851 19. Tanji T, Yun E-Y, Ip YT. Heterodimers of NF-κB transcription factors DIF and
852 Relish regulate antimicrobial peptide genes in Drosophila. Proceedings of the
853 National Academy of Sciences. 2010;107: 14715–14720.
854 doi:10.1073/pnas.1009473107

855 20. Ferrandon D, Jung AC, Criqui MC, Lemaitre B, Uttenweiler-Joseph S, Michaut L,
856 et al. A drosomycin-GFP reporter transgene reveals a local immune response in
857 Drosophila that is not dependent on the Toll pathway. EMBO Journal. 1998;17:
858 1217–1227. doi:10.1093/emboj/17.5.1217

859 21. Robinson SW, Herzyk P, Dow JAT, Leader DP. FlyAtlas: database of gene
860 expression in the tissues of Drosophila melanogaster. Nucleic Acids Research.
861 2013;41: D744–D750. doi:10.1093/nar/gks1141

862 22. Levy F, Rabel D, Charlet M, Bulet P, Hoffmann JA, Ehret-Sabatier L. Peptidomic
863 and proteomic analyses of the systemic immune response of Drosophila.
864 Biochimie. 2004;86: 607–616. doi:10.1016/j.biochi.2004.07.007

865 23. Tzou P, Reichhart J-M, Lemaitre B. Constitutive expression of a single
866 antimicrobial peptide can restore wild-type resistance to infection in
867 immunodeficient Drosophila mutants. Proceedings of the National Academy of
868 Sciences of the United States of America. 2002;99: 2152–2157.
869 doi:10.1073/pnas.042411999

870 24. Wiegand I, Hilpert K, Hancock REW. Agar and broth dilution methods to
871 determine the minimal inhibitory concentration (MIC) of antimicrobial
872 substances. Nature Protocols. 2008. doi:10.1038/nprot.2007.521

873 25. Rabel D, Charlet M, Ehret-Sabatier L, Cavicchioli L, Cudic M, Otvos L, et al.
874 Primary Structure and in Vitro Antibacterial Properties of the Drosophila
875 melanogaster Attacin C Pro-domain. Journal of Biological Chemistry. 2004;279:
876 14853–14859. doi:10.1074/jbc.M313608200

877 26. Rahnamaeian M, Cytry ska M, Zdybicka-Barabas A, Dobslaff K, Wiesner J,
878 Twyman RM, et al. Insect antimicrobial peptides show potentiating functional
879 interactions against Gram-negative bacteria. Proceedings of the Royal Society
880 B: Biological Sciences. 2015;282: 20150293–20150293.
881 doi:10.1098/rspb.2015.0293

882 27. Kragol G, Lovas S, Varadi G, Condie BA, Hoffmann R, Otvos L. The antibacterial
883 peptide pyrrhocoricin inhibits the ATPase actions of DnaK and prevents
884 chaperone-assisted protein folding. Biochemistry. 2001;40: 3016–3026.
885 doi:10.1021/bi002656a

886 28. Ryder E, Blows F, Ashburner M, Bautista-Llacer R, Coulson D, Drummond J, et
887 al. The DrosDel collection: A set of P-element insertions for generating custom
888 chromosomal aberrations in Drosophila melanogaster. Genetics. 2004;167:
889 797–813. doi:10.1534/genetics.104.026658

890 29. Ferreira ÁG, Naylor H, Esteves SS, Pais IS, Martins NE, Teixeira L. The Toll-
891 dorsal pathway is required for resistance to viral oral infection in Drosophila.
892 PLoS Pathog. 2014;10: e1004507. doi:10.1371/journal.ppat.1004507

893 30. Levashina EA, Ohresser S, Bulet P, Reichhart J -M, Hetru C, Hoffmann JA.
894 Metchnikowin, a Novel Immune-Inducible Proline-Rich Peptide from
895 Drosophila with Antibacterial and Antifungal Properties. European Journal of
896 Biochemistry. 1995;233: 694–700. doi:10.1111/j.1432-1033.1995.694_2.x

897 31. Fehlbaum P, Bulet P, Michaut L, Lagueux M, Broekaert WF, Hetru C, et al. Insect
898 immunity: Septic injury of drosophila induces the synthesis of a potent
899 antifungal peptide with sequence homology to plant antifungal peptides.
900 Journal of Biological Chemistry. 1994;269: 33159–33163.

901 32. Zhang Y, Zhao J, Fang W, Zhang J, Luo Z, Zhang M, et al. Mitogen-Activated
902 Protein Kinase hog1 in the Entomopathogenic Fungus Beauveria bassiana
903 Regulates Environmental Stress Responses and Virulence to Insects. AEM.
904 2009;75: 3787–3795. doi:10.1128/AEM.01913-08

905 33. Dudzic JP, Hanson MA, Iatsenko I, Kondo S, Lemaitre B. More Than Black or
906 White: Melanization and Toll Share Regulatory Serine Proteases in Drosophila.
907 Cell Reports. 2019;27: 1050-1061.e3. doi:10.1016/j.celrep.2019.03.101

908 34. Binggeli O, Neyen C, Poidevin M, Lemaitre B. Prophenoloxidase Activation Is
909 Required for Survival to Microbial Infections in Drosophila. PLoS Pathogens.
910 2014;10. doi:10.1371/journal.ppat.1004067

911 35. DeSimone SM, White K. The Drosophila erect wing gene, which is important for
912 both neuronal and muscle development, encodes a protein which is similar to
913 the sea urchin P3A2 DNA binding protein. Mol Cell Biol. 1993;13: 3641–3649.
914 doi:10.1128/MCB.13.6.3641

915 36. Elya C, Lok TC, Spencer QE, McCausland H, Martinez CC, Eisen M. Robust
916 manipulation of the behavior of Drosophila melanogaster by a fungal pathogen
917 in the laboratory. eLife. 2018;7: e34414. doi:10.7554/eLife.34414

918 37. Imler J-L, Bulet P. Antimicrobial peptides in Drosophila: structures, activities
919 and gene regulation. Chemical immunology and allergy. 2005;86: 1–21.
920 doi:10.1159/000086648

921 38. Hedengren M, Borge K, Hultmark D. Expression and evolution of the Drosophila
922 attacin/diptericin gene family. Biochemical and biophysical research
923 communications. 2000;279: 574–81. doi:10.1006/bbrc.2000.3988

924 39. Khush RS, Lemaitre B. Genes that fight infection: what the Drosophila genome
925 says about animal immunity. Trends Genet. 2000;16: 442–449.
926 doi:10.1016/s0168-9525(00)02095-3

927 40. Goto A, Yano T, Terashima J, Iwashita S, Oshima Y, Kurata S. Cooperative
928 regulation of the induction of the novel antibacterial Listericin by
929 peptidoglycan recognition protein LE and the JAK-STAT pathway. J Biol Chem.
930 2010;285: 15731–15738. doi:10.1074/jbc.M109.082115

931 41. Barajas-azpeleta R, Wu J, Gill J, Welte R. Antimicrobial peptides modulate long-
932 term memory. PLoS Genetics. 2018; 1–26. doi:10.1371/journal.pgen.1007440

933 42. Steffen H, Rieg S, Wiedemann I, Kalbacher H, Deeg M, Sahl H-G, et al. Naturally
934 processed dermicidin-derived peptides do not permeabilize bacterial
935 membranes and kill microorganisms irrespective of their charge. Antimicrob
936 Agents Chemother. 2006;50: 2608–2620. doi:10.1128/AAC.00181-06

937 43. Zdybicka-Barabas A, Mak P, Klys A, Skrzypiec K, Mendyk E, Fiołka MJ, et al.
938 Synergistic action of Galleria mellonella anionic peptide 2 and lysozyme against
939 Gram-negative bacteria. Biochim Biophys Acta. 2012;1818: 2623–2635.
940 doi:10.1016/j.bbamem.2012.06.008

941 44. Casteels-Josson K, Capaci T, Casteels P, Tempst P. Apidaecin multipeptide
942 precursor structure: a putative mechanism for amplification of the insect
943 antibacterial response. The EMBO journal. 1993;12: 1569–78.
944 doi:10.1002/j.1460-2075.1993.tb05801.x

945 45. Hanson MA, Hamilton PT, Perlman SJ. Immune genes and divergent
946 antimicrobial peptides in flies of the subgenus Drosophila. BMC evolutionary
947 biology. 2016;16: 228. doi:10.1186/s12862-016-0805-y

948 46. Koganezawa M, Haba D, Matsuo T, Yamamoto D. The Shaping of Male Courtship
949 Posture by Lateralized Gustatory Inputs to Male-Specific Interneurons. Current
950 Biology. 2010;20: 1–8. doi:10.1016/j.cub.2009.11.038

951 47. Kurz CL, Charroux B, Chaduli D, Viallat-Lieutaud A, Royet J. Peptidoglycan
952 sensing by octopaminergic neurons modulates Drosophila oviposition. Elife.
953 2017;6. doi:10.7554/eLife.21937

954 48. Lezi E, Zhou T, Koh S, Chuang M, Sharma R, Pujol N, et al. An Antimicrobial
955 Peptide and Its Neuronal Receptor Regulate Dendrite Degeneration in Aging
956 and Infection. Neuron. 2018;97: 125-138.e5. doi:10.1016/j.neuron.2017.12.001

957 49. Gramates LS, Marygold SJ, Dos Santos G, Urbano JM, Antonazzo G, Matthews BB,
958 et al. FlyBase at 25: Looking to the future. Nucleic Acids Research. 2017;45:
959 D663–D671. doi:10.1093/nar/gkw1016

960 50. Hill T, Koseva BS, Unckless RL. The genome of Drosophila innubila reveals
961 lineage-specific patterns of selection in immune genes. Molecular Biology and
962 Evolution. 2019. doi:10.1093/molbev/msz059

963 51. Chambers MC, Jacobson E, Khalil S, Lazzaro BP. Thorax injury lowers resistance
964 to infection in Drosophila melanogaster. Infect Immun. 2014;82: 4380–4389.
965 doi:10.1128/IAI.02415-14

966 52. Verleyen P, Baggerman G, D'Hertog W, Vierstraete E, Husson SJ, Schoofs L.
967 Identification of new immune induced molecules in the haemolymph of
968 Drosophila melanogaster by 2D-nanoLC MS/MS. Journal of Insect Physiology.
969 2006;52: 379–388. doi:10.1016/j.jinsphys.2005.12.007

970 53. Pfaffl MW. A new mathematical model for relative quantification in real-time
971 RT-PCR. Nucleic Acids Res. 2001;29: e45. doi:10.1093/nar/29.9.e45

972 54. Tyler-Cross R, Schirch V. Effects of amino acid sequence, buffers, and ionic
973 strength on the rate and mechanism of deamidation of asparagine residues in
974 small peptides. J Biol Chem. 1991;266: 22549–22556.

975
976

977 ## Supplemental figure and table captions:

978

979 **Figure S1: Supplemental *BaraA* expression patterns. A)** 400bp of upstream
980 sequence from *BaraA* annotated with putative *Rel* or *Dif/dl* binding sites (included
981 in supplemental data file 1). **B)** Expression of *BaraA in wild-type* and *spz^{rm7} flies*
982 following injury with the Gram-positive bacteria *M. luteus* . **C)** The *BaraA>mGFP*
983 reporter line shows a robust induction of GFP 2hpi upon pricking with *M. luteus* in
984 larvae. **D)** Expression of *BaraA>mGFP* in the spermatheca of females (yellow arrow).
985 Representative images shown.

986

987 **Figure S2: LCMS coverage of trypsin-digested and detected BaraA peptides**
988 **aligned to the protein coding sequence.** Peptide fragments cover the whole
989 precursor protein barring furin site-associated motifs. Additionally, two peptide
990 fragments are absent: i) the first 4 residues of the C-terminus ("GIND," not predicted
991 *a priori*), and ii) the C-terminus peptide's "RPDGR" motif, which is predicted as a
992 degradation product of Trypsin cleavage and whose size is beyond the minimum
993 range of detection. Without the GIND motif, the mass of the contiguous C-terminus is
994 5974.5 Da, matching the mass observed by MALDI-TOF for IM22 (**Fig.** 2A). The N-
995 terminal Q residues of IM10, IM12, IM13, and IM24 are pyroglutamate-modified, as
996 described previously [22]. The asparagine residues of IM10-like peptides are
997 sometimes deamidated, likely as a consequence of our 0.1% TFA sample collection
998 method as "NG" motifs are deamidated in acidic conditions [54].

999

1000 **Figure S3: Alignments of BaraA peptide motifs. A)** Aligned IM22 peptides of
1001 *Drosophila Baramicin A-like* genes, with the IM10-like 'VWKRPDGRTV' motif noted.
1002 The GIND residues at the N-terminus are cleaved off in *Dmel\BaraA* by an unknown
1003 process, and this site is similarly cleaved at RXRR furin cleavage site in subgenus
1004 Drosophila flies. As a consequence, the mature IM22 peptide is predicted to be the
1005 same across species even when different cleavage mechanisms are utilized. **B)**
1006 Alignment of the three IM10-like peptides of *D. melanogaster BaraA* with the
1007 "VXRPXRTV" motif noted.

1008

1009 **Figure S4: *Over-expression of BaraA partially* rescues *Rel, spz* double mutant**
1010 **susceptibility to infection in both males and females. A)** validation of the *UAS-*
1011 *BaraA* construct in the *Rel, spz* background. **B)** Overexpressing *BaraA* did not
1012 improve the survival of *Rel, spz* flies upon *E. coli* infection. **C)** Overexpressing *BaraA*
1013 only marginally improves survival of *Rel, spz* females, but not males, upon *M. luteus*
1014 infections. Infections using a higher dose tended to kill 100% of *Rel, spz* flies
1015 regardless of sex or expression of *BaraA*, suggesting that if *BaraA* overexpression
1016 does affect susceptibility to *M. luteus*, this effect is possible within only a narrow
1017 window of *M. luteus* concentration. **D-F)** Overexpressing *BaraA* improves survival of
1018 *Rel, spz* male and female flies upon injury with *C. albicans* **(D)** or natural infection
1019 with *A. fumigatus* **(E)** and *N. crassa* **(F).** P-values are shown for each biological sex in
1020 an independent CoxPH model not including the other sex relative to *Rel, spz* as a
1021 reference.

1022
1023 **Figure S5:** RT-qPCR shows that the expression of *BomBc3* **(A)** *Drs* **(B)** and *DptA* **(C)**
1024 is wild-type 18hpi in *iso ΔBaraA* flies. **D)** *BaraA* mutants survive clean injury like
1025 wild-type flies. **E)** *iso ΔBaraA* flies have similar lifespan compared with the *iso* w^{1118}
1026 wild-type (males + females, *iso vs. iso ΔBaraA*: HR = 0.26, p = .118).
1027
1028 **Figure S6: Additional survivals using *ΔBaraA* flies in two distinct genetic**
1029 **backgrounds upon infection by a diversity of microbes. A)** No significant
1030 susceptibility of *ΔBaraA* flies to *Ecc15* infection. **B)** *w; ΔBaraA but not iso ΔBaraA*
1031 flies exhibit a marginal susceptibility to *B. subtilis* (HR > 0.5, p = .099). **C-D)** *w;*
1032 *ΔBaraA* males were slightly susceptible to *A. fumigatus* natural infection (HR > 0.5, p
1033 = .078), but not females, nor isogenic flies. Additional infections using *ΔBaraA,*
1034 $Bom^{\Delta 55C}$ double mutant flies reveal that *BaraA* mutation increases the susceptibility
1035 of $Bom^{\Delta 55C}$ flies in both males and females (cumulative curves shown in **Fig.** 5A).
1036 Blue backgrounds = Gram-negative bacteria, orange backgrounds = Gram-positive
1037 bacteria, yellow backgrounds = fungi.
1038
1039 **Figure S7: Additional survival analyses reveal only a minor contribution of**
1040 ***BaraA* to defence against infection by *E. faecalis*. A)** Crosses with a genomic
1041 deficiency (*Df(BaraA)*) leads to increased susceptibility in both the *w* background
1042 and isogenic DrosDel background, with *Df(BaraA)/ΔBaraA* flies suffering the
1043 greatest mortality in either crossing scheme. Both deficiency crosses yielded an
1044 earlier susceptibility in *BaraA*-deficient flies (shown with dotted black lines),
1045 however neither experiment ultimately reached statistical significance. **B)** *BaraA*
1046 RNAi flies (*Act>BaraA-IR*) suffered greater mortality than *Act>OR-R* or *OR-R/BaraA-*
1047 *IR* controls, but this was not statistically significant at α = .05; p-values reported are
1048 comparisons to *Act>BaraA-IR* flies.
1049
1050 **Figure S8: Additional survival analyses reveal a consistent contribution of**
1051 ***BaraA* to defence against natural infection with *B. bassiana*. A)** Crossing with a
1052 genomic deficiency (*Df(BaraA)*) leads to increased susceptibility of
1053 *Df(BaraA)/ΔBaraA* flies for both the *w* background and isogenic DrosDel
1054 background relative to wild-type controls (p < .05). **B)** *Act>BaraA-IR* flies were more
1055 susceptible than the *OR-R* wild-type (p = .008) and *OR>BaraA-IR* (p = .004), although
1056 not significantly different from our *Act>OR-R* control (p = .266). **C)** Overexpressing
1057 *BaraA* (*Act>UAS-BaraA*) improved survival against *B. bassiana* relative to *Act>OR-R*
1058 controls (HR = -0.52, p = 0.010).
1059
1060 **Figure S9: Frequency of erect wing display following additional challenges. A-**
1061 **B)** Erect wing frequencies 2dpi after clean injury **(A)**, or *Ecc15* septic injury **(B)**. The
1062 erect wing frequencies of flies pricked by HK-*E. faecalis* (**Fig.** 6D) are included in
1063 brown in **A** and **B** to facilitate direct comparison with the frequency observed upon
1064 Toll pathway activation. **C)** The frequency of erect wing display is increased
1065 following *E. faecalis* septic injury in *ΔBaraA/+* or *Df(BaraA)/+* flies. Data points are
1066 pooled from *w; ΔBaraA* and *iso ΔBaraA* crosses after *E. faecalis* infections shown in
1067 **Fig.** S7A and data in **Table** S1.

1068
1069 **Table S1: Erect wing frequencies from various infection experiments.**
1070 Following initial erect wing observations upon *A. fumigatus* natural infection, we
1071 scored erect wing frequency in all subsequent survival experiments. Data represent
1072 the mean % of males displaying erect wing ± one standard deviation. n exp =
1073 number of replicate experiments performed, and dpi ewg taken = days post-
1074 infection where erect wing data were recorded. We additionally performed natural
1075 infections with *Metarhizium rileyi* that generally did not cause significant mortality
1076 even in *ΔBaraA, Bom*$^{\Delta 55C}$ double mutant males, but nevertheless induced erect wing
1077 specifically in *ΔBaraA* males and *spz*^{rm7} controls. Bacterial infections were
1078 performed by septic injury, while fungal challenges were natural infections
1079 performed by rolling flies in spores.
1080

1081 **Supplementary information:**
1082
1083 ***Identification of the BaraA C-terminus as IM22 from Uttenweiler-Joseph et al.***
1084 In 1998, Uttenweiler-Joseph et al. [8] described 24 immune-induced
1085 molecules by MALDI-TOF and informed predictions suggested that *BaraA* could
1086 encodes several of them [22]. We generated a knock out mutant for the *BaraA* gene
1087 ($BaraA^{SW1}$), which we validated by MALDI-TOF peptidomic analysis. Strikingly, we
1088 noticed an immune-induced peak at ~5981 Da in Linear mode collections that is
1089 absent in *ΔBaraA* flies (**Fig.** 2A); this mass closely resembled the 5984 Da estimated
1090 mass of IM22 from Uttenweiler-Joseph et al. [8], for which sequence was never
1091 determined. We took the Linear masses reported for then-unknown IMs from
1092 Uttenweiler-Joseph et al. [8] and post-hoc generated a standard curve with now-
1093 confirmed mass values from Levy et al. [22]. Our post-hoc standard curve corrects
1094 the mass of IM22 as found in Uttenweiler-Joseph et al. [8] to be 5973.5 Da. Using the
1095 same approach with our own linear data we find a mass of 5975.1 Da for our 5981
1096 Da peak (supplementary data file 1). With LCMS proteomics, we confirmed that the
1097 *BaraA* C-terminus is cleaved to remove 4 N-terminal residues, which should produce
1098 a putative 5974.5 Da peptide (**Fig** S2). Together these observations indicate the
1099 *BaraA* C-terminus encodes the following 53-residue mature peptide, matching the
1100 estimated mass of IM22: ARVQGENFVA RDDQAGIWDN NVSVWKRPDG
1101 RTVTIDRNGH TIVSGRGRPA QHY.
1102
1103 The *BaraA* gene is therefore involved in the production of over one third of
1104 the classical *Drosophila* IMs from Uttenweiler-Joseph et al. [8], including: IM5, 6, 8,
1105 10, 12, 13, 20 (doubly-charged IM24 [22]), 22, and 24.
1106
1107
1108
1109
1110
1111

Sequence of the BaraA-Gal4 promoter construct

The following 1675bp sequence was cloned from the DrosDel isogenic background into the pBPGUw vector to drive a downstream Gal4 gene, and inserted into the VK33 attP docking site using BDSC line #24871:

Dif/dorsal binding site **(bold)***:* **GGGHHNNDVH**

Rel binding site (underline): GGRDNNHHBS

>iso_DrosDel_BaraA_promoter-Gal4

CTGCTACTCCTCTACACATTCGACTCCTTCGCCTTGCTGGCTGGGAAAAAATTTTGCATA
ATTTATGTGGGTGCCGCGCACACGGAGGTCCCGACGGATTCGAAGTATCCGAAGGATTCG
AAAGGAAAACAACGCACGAGCACCACGGCCAACTGATTTAAATGCAATTGCACTGAAGT
ATTTTGTTTGGCGAACGAAGCTGGATGAAATAGGGGGGTGTGGGGTTTTCTATTGAGAC
ATCTGCACGTGCAACCGGAAACATCCGAAGAGAACAGCACAGGCCGGGCTACGCCGGGCA
ATTTCTTTTCATTTGCCAAGGTGTTGAGTTGCACCAACATTCGACATCGACGTGGCCAGA
AGCCAACAAAAGCCAAGAGCCAAACCCCTTTTTGTGGTCACAAGTGTCGTCTATTTGTCG
TGGGCATCTTGGGCACCTTGGGCATCCTCGACATCCTTGCCATTTTGGTCTGGCCAAGAC
AAACAACCAGCAAATTTAGTGTATTTTGTGCATTTTTAAAATTGTCCAAATTTATGTGA
CACGCTGCGCCAATTGATCAGATTAAATAAACATGAGGCCAAGCGAATCGAATTTGGCTT
CACCAAGAAGACAATGCAGTCTGTATTCAAATGGGTGGGCGCATCCACCAAGCGGTGAAT
ACAGTGACCGCTCGCTATAATGGACGGTCAGGTGTTACTTTAACTTAAAAAAATATGTA
ACAAATCTTATCAAGTTTGAAATAGATTGAAATAGATTTGGTTATTGCATTCGAAAGAT
ATATATTAAATTCGAATATTCCAAGAAATTTCATGAGAATGTCACTTATGTCATGAGAT
TATATTAACGTACGAATAAACAATGTATTTTCCAAAATTAAAAATAAAATTTAATTTAA
TTACGCAGTACCTTTACACTATCAGTCGGAGGTAATAACTCATATAATTAGATTAGCATT
AGATTTTAAAGCGAAAAACACTTAAAAGCTGAAATTATTAGACAACACTCTTAAATTAG
TCGAGCTGATATATAGCCTCAAGTTTTGCTTAAATCCAAAGATAAAGGAATGCCTTCAA
AAATATATTTTGTTTTATACCAAGTGACAGCAGAGAATGGGGTTGCAATATCTTAAAAG
AGTTTCACTTAGCCAATATTTACTGCCATTGTTGGCCACCAAATAGTAGCAACCAGAGAC
TTCCAGGAATATATTCTCGTGTCAAATGCAATCCACTTTAAATGCAACTATCTGGCGGCT
AAGAAAACCCGACAGTTTGATTCAAGTCGACGAAACAATATAAGCACGTGCTAAATAAA
GAGACCTATGCAGTTAATACTCTTGTCATATTATAATATAATTTAGTGACATAAGTTGC
ATGGTATACGAGTACTGAACAAGTTATGGCAGCTTTTCCAAATAAGCGATCACATATTCC
GCGGGATGATGGGTGGATTTCTAGCATATGTGGATGCTTAATGGCTTATTGC**GGGTCAG**
GGCGGCGCAATCTGTTC**AGAAATTCCC**GAACGCACACCCATTTCAGATCAGATTGTGAC
GTTTT**GGGAAATTCT**TGACGATCGGTGTAAACAAGCTCAGCAACCAGATTCGATGGCTA
TTTGCCGGCTATAAATACTAGAAACCATTCGATTGCACTCAGTTGAAGCTGGGCTCTGGA
ACAGATCACA